

A High-Speed Differential Thermographic Camera

Jon R. Lesniak
Bradley R. Boyce

Stress Photonics Inc.
565 Science Drive
Madison, WI 53711

Abstract

Advanced infrared array-detector technology and high-speed digital processing have been combined to dramatically improve the applicability of thermoelastic stress analysis. Details of the implementation of a 128 x 128 InSb focal-plane-array detector for imaging dynamic stresses in structures is described. A comparison of system design parameters between single-detector scanning systems and staring-array systems describe the orders of magnitude improvement in imaging speed provided by array technology. Performance parameters are explained for a broad range of specimen temperatures showing the ease with which the array system can be adapted for elevated temperature stress analysis and material characterization.

Introduction

Roughly ten years ago the first commercially available differential thermography system for Thermographic Stress Analysis (TSA) was introduced (SPATE¹ by Ometron). Recently, a NASA-Langley funded development effort has moved this technology ahead in a dramatic way. This paper introduces an improved device that has shortened the time to collect a TSA image by three orders of magnitude while reducing the system's size, weight, and complexity. The improved imaging speed, accomplished through the combination of array detector technology and high-speed

digital processing, provides instantaneous stress images under most common structural loading.

Thermoelastic Stress Analysis, TSA is able to image dynamic stresses in a structure by measuring the small temperature changes that occur when a material is compressed or expanded. The magnitude of these changes is generally quite small, in steel for instance 1.0 mK is the equivalent of a stress change of 1.0 MPa (150 psi). Only the exquisite sensitivity of modern detectors combined with sophisticated electronics and signal processing has made it possible to design imaging systems that provide a useful level of thermal, and hence, stress resolution.

A newly developed system can reduce average acquisition time for a TSA image from 30 minutes to 15 seconds. Signal-to-noise calculations presented in this paper indicate that a factor of 1600 speed improvement is obtainable. The new system also provides rough stress images instantaneously on a standard video monitor. This rapid feedback coupled with the system's "video camera like" ease of operation has accelerated the development of TSA as an experimental stress analysis method. In this paper practical application of TSA for the characterization of material specimens during room and elevated temperature testing is described and gives evidence of the rapid maturation of TSA.

Thermoelastic Stress Analysis Primer

Thermoelastic Stress Analysis (TSA) is a full-field, non-contacting stress-analysis technique. Infrared cameras can be used to measure the small, load-induced temperature changes (ΔT) described by

$$\Delta T = \frac{T}{C_p} \left(\epsilon_x + \nu \epsilon_y \right) \quad (1)$$

¹ SPATE is an acronym for Stress Pattern Analysis by Thermal Emission. It is considered by many individuals involved in the study of thermoelasticity as being synonymous with high-resolution infrared detection. Thus, SPATE camera and SPATE measurements are examples of terminology that have frequently been adopted in TSA research and development.

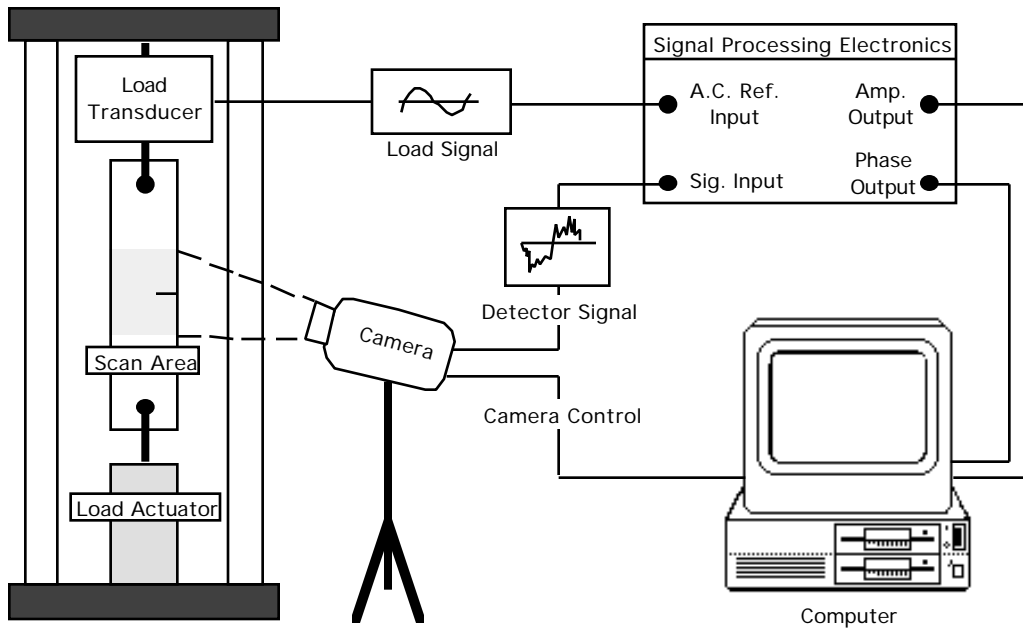


Fig. 1 TSA system block diagram

where ρ is the density, α is the thermal expansion coefficient, C_p is the specific heat, T is the absolute temperature and σ_x and σ_y are the normal stress components. These cameras are referred to as differential thermographic cameras. To improve measurements, the temperature changes induced by the thermoelastic effect are repeated and time-averaged with continuous dynamic loading. Although sinusoidal loading is most common, more complex load histories like those used in load simulators or actual service loads can be used. Figure 1 is a block diagram of a typical laboratory setup. A closed-loop hydraulic load frame provides the loading while a TSA system correlates the load-induced IR signals with the reference signal from the load cell or strain gage.

Slow Scan Mirror Differential Thermographic Camera

The "slow scan" TSA camera uses a single HgCdTe detector. It employs mirrors to raster scan the surface of the component, aiming at each point for up to 0.5 second while correlating the IR signal with the reference via an analog lock-in amplifier[1]. This system is slow, taking from 15 minutes to several hours per scan. Its thermal-differential resolution is on the order of 1.0 mK. Ometron of London, England makes the line of slow scan TSA cameras.

Video Scan Mirror Differential Thermographic Camera

A few organizations have adapted standard infrared cameras for TSA measurement[2]. Typically these cameras have scanning mirrors that move at video rates to produce DC thermal images that can easily be displayed by a standard video monitor and digitized by off-the-shelf computer hardware. The adaptation for TSA of a camera with mirrors that scan at video rates is simple if the dynamic stress in the structure has a frequency well below the framing rate (usually 25-30 frames/second). Above or near the framing rate, special interlaced or aliased sampling techniques must be used. But, no matter how fast the mirrors scan, if the camera has only one detector, then for the purposes of this discussion it is essentially the same as the slow scan camera described above. From here on these cameras will simply be referred to as scanning TSA cameras.

Staring-Array Differential Thermographic Camera

Many types of infrared detector arrays are available, but the most appropriate for differential thermography is an InSb focal plane array (FPA). Stress Photonics has developed a 128 x 128 InSb FPA based camera for differential thermography under funding from NASA-Langley NDE Sciences Branch. A working prototype has recently become available and was used to verify the following discussion and provide the examples found toward the end of the paper.

The average InSb detector of the prototype array system is nearly an order-of-magnitude less sensitive than the single HgCdTe detector of the SPATE system, but because there are 16384 detectors in the array, a factor of about 1600 increase in overall imaging speed can be realized. This is because the array detectors can average out noise by staring at their respective sample areas for the entire acquisition time, about 10 seconds, where the slow-scan camera's detector only samples each area for a fraction of a second. To assure that the advantage of having 16384 sensors all working in parallel is not lost to a bottleneck in signal processing special high-speed digital electronics was developed to process the incoming signals at frame rates up to 1000 frames/second. To fully understand the staring-array camera's ability to achieve signal to noise ratios as good or better than the single-detector, scanning-mirror camera one must have a basic understanding of the relationship between the measurement equipment and the differential thermal signal.

The array camera correlates the IR signals digitally described by the relation

$$B = \frac{2}{N} \sum_{n=1}^N y_n \sin(n) \quad (2)$$

where B is the amplitude of the signal, y_n is the sampled signal, N is the number of samples, and $\sin(n)$ is a reference.

General Camera/TSA Theory

An infrared camera converts each photon strike into an electrical event. In the case of photovoltaic detectors, each registered photon strike is converted into a charge. The rate at which these charges are generated is a current. The detector output is proportional to the rate of photons striking it, the photon incidence. There are three important quantities to understand when designing a thermographic system: the background photon incidence b_b , the signal incidence b_s , and the noise-equivalent photon rate.

Background Photon Incidence

The rate at which photons are registered by the detector, or the background photon incidence b_b , is a function of the radiance of the specimen Q_b , the optics of the system, and the geometry of the detector,

$$b_b = \eta Q_b A_{det} \Omega_{cs} \quad (3)$$

where η is the quantum efficiency of the detector, Q_b is the background photon radiance, A_{det} is the area of the detector,

and Ω_{cs} is the solid angle of the optical system as properly defined by the cold shield (Fig. 2).

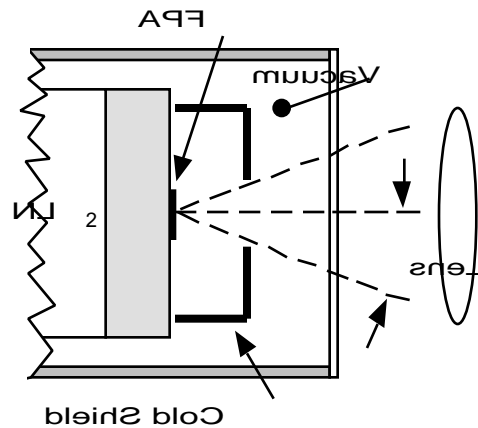


Fig. 2 Array camera optics.

The solid angle is defined as

$$\Omega_{cs} = 4 \pi \sin^2(\theta/2) \quad (4)$$

The background photon radiance Q_b is calculated from the spectral background photon radiance Q obtained by dividing Planck's Law by the energy per photons. The spectral photon radiance is converted from hemispheres to steradians by dividing by 2. The background radiance Q_b is defined by the integral

$$Q_b = \int_0^{\lambda_c} Q d\lambda \quad (5)$$

where

$$Q = \frac{c}{4} \frac{1}{\exp\left(\frac{ch}{kT}\right) - 1} \quad (6)$$

The spectral radiances for a range of temperatures are plotted in Fig. 3. Notice that as the temperature increases the peak wavelength shifts to the left. As the wavelength of the IR light increases, the energy per photon decreases. Photons of light beyond a certain wavelength do not carry sufficient energy to register. This is referred to as the cutoff wavelength of the detector. Assuming perfect transmittance over the spectrum the photon radiance measurable by the detector is the integral described by Eq. 5 up to the cutoff wavelength.

In actual practice, optical filters will be used to select a narrower band of light. InSb detectors, as used in the staring-array camera, make use of an IR spectral band of 3-5

microns, and HgCdTe as used in slow scan mirror camera, usually utilizes a spectral band of 8-12 microns. The photon radiance is the integral over the spectral bandwidth between λ_1 and λ_2 .

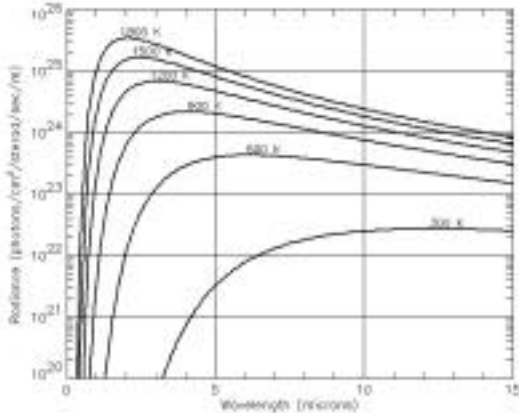


Fig. 3 Spectral background photon radiance

The array camera integrates the charges generated by the photon incidence in a quantum well. The number of charges stored in the well per frame is

$$b = b \cdot t \tag{7}$$

where t is the integration time. Often the integration time is the inverse of the frame rate of the camera.

Signal Photon Radiance

The signal photon radiance Q_s is the increase in photon incidence from a small temperature change. The thermal changes generated by the thermoelastic effect (Eq. 1) are very small compared to the absolute temperature of the body. This implies that the change in the photon radiance of the body due to the imparted stress is also very small compared to the background photon radiance. The signal photon radiance for T can be determined by calculating the difference of background photon radiance for temperatures T and $T + \Delta T$.

$$Q_s = 0.71 \int_0^\infty (\tau(\lambda) (Q(T + \Delta T) - Q(T))) d\lambda \tag{8}$$

where τ is the spectral transmittance. The spectral signal photon radiance for $T=1.0$ mK is plotted in Fig. 4.

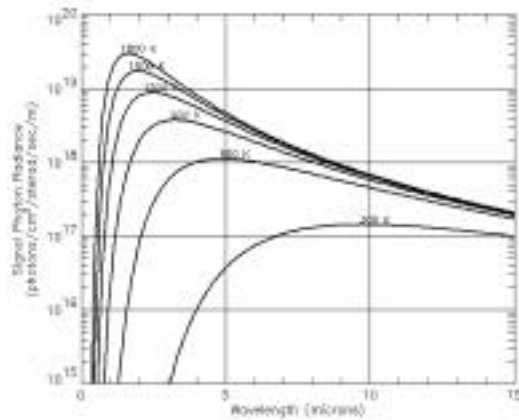


Fig. 4 Spectral signal photon

Again, as the temperature increases, most of the signal photons are emitted at the lower wavelengths. The signal photon radiance of a bandwidth is calculated in the same manner as for the background photon radiance.

Similar to the calculation of the background photon count, the root-mean-square signal photon count is

$$s = 0.707 \cdot s \cdot t \tag{9}$$

Fig. 3 and Fig. 4 show that the signal radiance is about 1/100,000 of the background radiance. Even the 12 bit A/D's common to most off-the-shelf IR cameras can not resolve this accuracy. Although some improvement in digital resolution is achieved by signal processing, several bits worth is not easily obtained. Therefore, a patented high-speed offset technique is implemented where each detectors background radiance is offset before sampling. This provides higher resolution as the A/D is set up to span only the signal range. The offsets are calculated on a per detector basis and are updated continuously.

Background-Limited Noise

The detector noise is proportional to the variations in the background photon radiance caused by the randomness of the photon emission from the surface of the structure. A background-limited infrared photodetector (BLIP) is sufficiently cooled so that thermoelectric noises are insignificant; therefore, noise models are based primarily on the stochastic photon emissions. The noise-equivalent photon rate (NEPR) of a photovoltaic detector is

$$NEPR_{rms} = (2 \cdot b \cdot f)^{-1} \tag{10}$$

where f is the noise-equivalent bandwidth[3]. The NEPR is the rate of signal photons required to match the noise rate

thus making the signal-to-noise ratio unity. The noise equivalent photon count (NEPC) can be calculated from the NEPR by

$$\text{NEPC}_{\text{rms}} = \text{NEPR}_{\text{rms}} t \quad (11)$$

For the purpose of noise and signal-to-noise ratios calculations, the following specifications are used for all calculations of performance of camera system.

$$\begin{aligned} \omega_{\text{cs}} &= .087 \text{ster} (f/3) \\ A_{\text{det}} &= 40 \mu\text{m} \times 40 \mu\text{m} \\ &= 1 \\ f &= 1 \end{aligned} \quad (12)$$

The SPATE system varies slightly from these specifications.

In Eq. 10 the noise of a BLIP is related to the root of the noise-equivalent bandwidth. For a time-integrated sample the noise bandwidth is

$$f = \frac{1}{2t} \quad (13)$$

Substituting the relation for NEPR of Eq. 10 and the noise-equivalent bandwidth of Eq. 13 into Eq. 11 yields.

$$\text{NEPC}_{\text{rms}} = \left(\frac{s}{b} \right)^{\frac{1}{2}} \quad (14)$$

Thus, it is apparent by Eq. 14 that the NEPC is related solely to the background photon count. The NEPC serves as the root-mean-square noise per sample, or in terms of digitized samples, it is the standard deviation of the sample.. The signal to noise ratio is defined

$$\text{S/N} = \frac{s}{\text{NEPC}} \quad (15)$$

The signal calculations up to this point have been based on a fixed thermal signal of 1.0 mK; however, the temperature change due to the thermoelastic effect is proportional to the absolute temperature of the specimen; this significantly improves the signal-to-noise ratio. The signal-to-noise ratio for thermoelasticity, accounting for the increased thermal signal due to elevated temperature, is plotted in Fig. 5. The signal-to-noise ratio of Fig. 5 are calculated considering the spectral bands used by each detector, and assume a f of 1.0 Hz. The data plotted in Fig. 5 represent ideal limits; at extreme temperatures there are some additional considerations involving array camera details that are not discussed here.

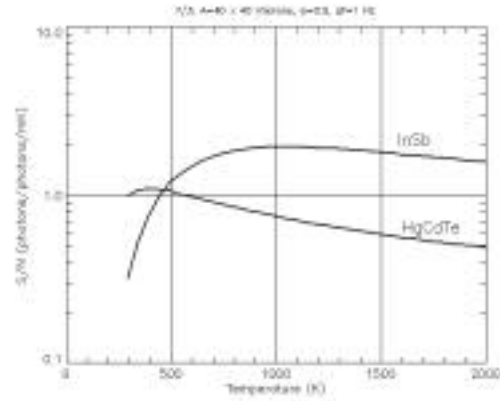


Fig. 5 S/N of InSb compared to HgCdTe vs. temperature.

Scan Time

The standard deviation (NEPC') of the end measurement B described by Eq. 2 is related to the standard deviation of each sample (NEPC),

$$\text{NEPC}' = \frac{\text{NEPC}}{\sqrt{N}} = \frac{\text{NEPC}}{\sqrt{R_F t_s}} \quad (16)$$

where t_s is the total scan time and R_F is the frame rate of the camera. In order to determine the scan time necessary to obtain a specific thermal resolution, the NEPC' is set to the value of the signal photon count for 1.0 mK,

$$\text{NEPC}' = s_{1.0\text{mK}} \quad (17)$$

Relation 18 is rearranged,

$$t_s = \frac{\text{NEPC}'^2}{s^2 R_F} = \frac{1}{R_F (\text{S/N})^2} \quad (18)$$

From Eq. 18, the ratio of the scan times required to achieve two signal-to-noise ratios can be determined,

$$\frac{t_2}{t_1} = \left(\frac{\text{S/N}_2}{\text{S/N}_1} \right)^2 \quad (19)$$

With this relation the scan time required for the staring-array camera to achieve 1.0 mK resolution can be calculated by reading the signal-to-noise ratio for 1.0 mK from Fig. 5. A 1.0 Hz noise-bandwidth is equivalent to 250 samples at a 500 Hz frame rate because as long as the samples are contiguous they result in the same noise reduction as one continuous integration time. Therefore,

$$t_{1.0mK} = \frac{(S/N)_{1.0mK}^2}{(S/N)_{f=1.0Hz}} t_{f=1.0Hz} = 10(0.5s) = 5.0s \quad (20)$$

So, in 5 seconds the staring array camera matches the signal-to-noise ratio of the slow scan camera. After 5.0 seconds the entire image has been acquired!

For a similar size image, the scan time for the slow scan system is 0.5 seconds x 16000 which is 8000 seconds. Therefore the speed improvement of the array system over the scanning system is a factor of 1600. The same 1.0 mK resolution stress image provided by SPATE in an hour can be captured in seconds with the staring array camera.

Staring-Array TSA Image Examples

The array camera is in its infancy, so the initial data does not reflect the array's full potential. A significant amount of noise reduction will be realized when the wire-wrap prototype boards are replaced with printed circuit boards (PCB's). Also, the data shown does not benefit from the use of a non-uniformity correction map. A non-uniformity correction map calibrates the variance in the sensitivities of the multitude of detectors present in the array.

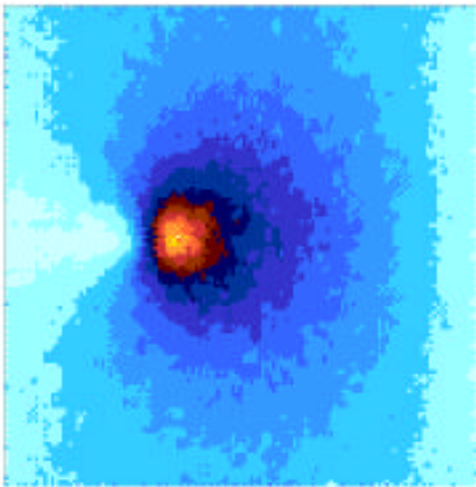


Fig. 6 Example TSA image from array camera. Crack tip of 1.5 mm thick aluminum (15 s acquisition time)

The implementation of a staring array camera for differential thermography provides a number of practical benefits beyond speed. For instance, a staring array camera can easily provide live DC thermography of the subject specimen. (Of course, the DC images can be quite useful in applications other than stress analysis.) The DC image

viewed on a video monitor facilitates aiming and focusing, and the DC image provides excellent documentation of the test set-up.

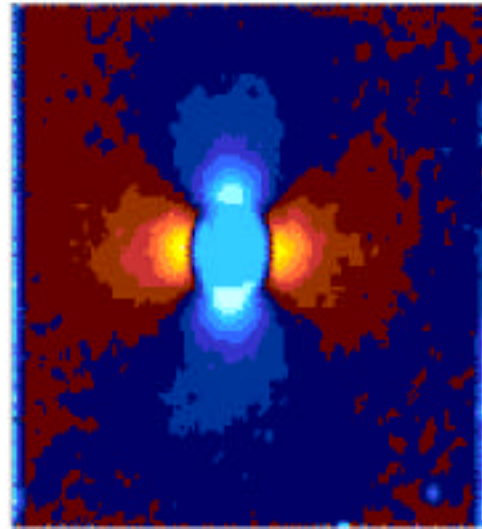


Fig. 7 Aluminum strap in vertical tension. Nominal stress is 42.0 MPa (6100 psi). The strap is 32 mm wide by 6 mm thick with a 6 mm hole. Image has been median filtered. Acquisition time: 16 s.

Since TSA and DC images are acquired simultaneously they can be overlaid to highlight the structure's physical geometry while at the same time showing the surface stress pattern, Fig. 8.

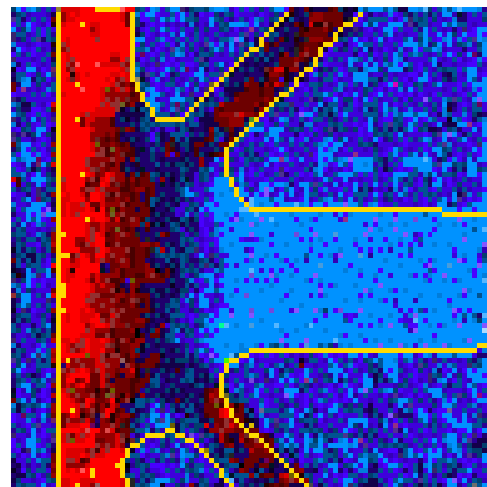
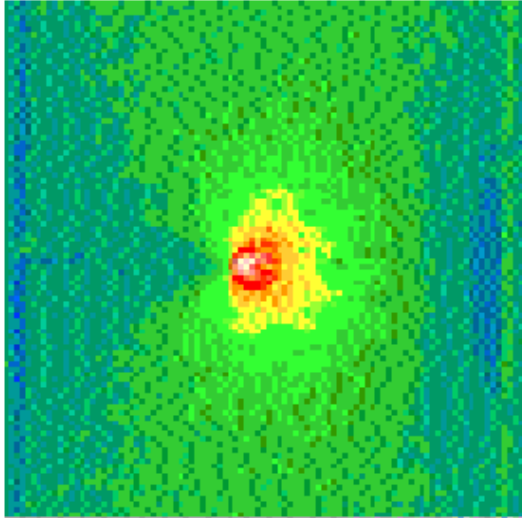
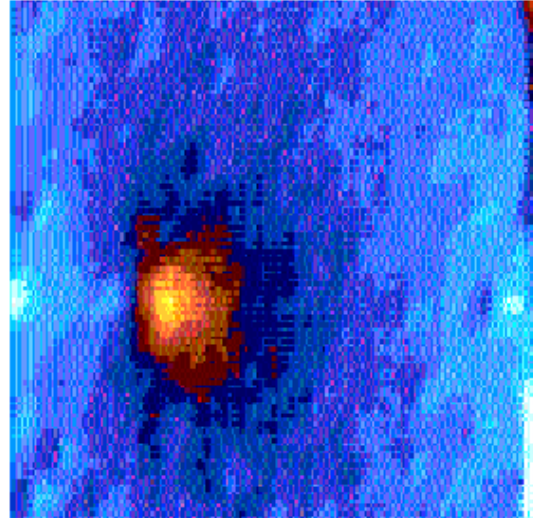


Fig. 8 DC image outline superimposed on the TSA image of an aluminum structure. Image acquisition time: 10 s.



(a) room-temperature TSA image



(b) high-temperature 480°C (900°F) TSA image

Fig. 9 TSA images of crack tip in 1.5mm (0.060") steel.

Fig. 9 exemplifies the array camera's ability to operate at elevated temperatures. These images were collected as a result of a Air Force funded effort to show the feasibility of elevated temperature TSA for stress analysis, and damage characterization. In the study the array camera was used to monitored crack growth with its one-second imaging capability.

Concluding Remarks

The development of an differential thermography system based on advanced array detector technology without the constraint of using off-the-self imaging and signal processing has lead to a dramatic improvement in system performance. The new system can nearly instantaneously present pseudo-color images of the dynamic stress in a structure. Furthermore, the physical implementation of a staring array for differential thermography leads to a number of important benefits beyond raw speed. In an array based system there are no moving parts so reliability is high. The elimination of mirror motors results in reduced weight and size. The few optical elements required for a staring array makes the best use of the available light (signal) and makes adapting the optics for special purposes as simple as possible.

Thermographic Stress Analysis will take a giant step forward as this new array-detector technology becomes available. We think the capability to easily make nearly instantaneous full-field stress maps will make TSA an essential engineering tool.

References

1. Oliver, D. E., "Stress Pattern Analysis by Thermal Emission," Chapter 14, Handbook of Experimental Mechanics, edited by A.S. Kobayashi, Prentice-Hall.
2. Welch, Christopher S., Cramer, Elliott K., Dawicke, David S., "Thermographic Inspection of Fatigue Cracks in Riveted Plates," Proc. of SEM Spring Conf., Milwaukee, Wisconsin, June 1991, pp 239-243.
3. Dennis, P.N.J., *Photodetectors: An Introduction to Current Technology*, New York: Plenum Press, 1987.